PHYSICAL REVIEW D **91,** 036007 (2015)

Full simulation of chiral random matrix theory at nonzero chemical potential by complex Langevin

A. Mollgaard
Niels Bohr Institute, University of Copenhagen, Blegdamsvej 17, 2100 Copenhagen Ø, Denmark

K. Splittorff
Discovery Centre, Niels Bohr Institute, University of Copenhagen, Blegdamsvej 17, 2100 Copenhagen Ø, Denmark

(Received 23 December 2014; published 26 February 2015)

It is demonstrated that the complex Langevin method can simulate chiral random matrix theory at nonzero chemical potential. The successful match with the analytic prediction for the chiral condensate is established through a shift of matrix integration variables and choosing a polar representation for the new matrix elements before complexification. Furthermore, we test the proposal to work with a Langevin-time-dependent quark mass and find that it allows us to control the fluctuations of the phase of the fermion determinant throughout the Langevin trajectory.

DOI: 10.1103/PhysRevD.91.036007 PACS numbers: 11.30.Rd, 11.30.Hv

I. INTRODUCTION

First principles nonperturbative simulations of full QCD have been limited to the region with small ratio of the quark chemical potential over temperature or heavy quark masses because of the fermion sign problem; for reviews see [1–3]. Recently, however, complex Langevin simulations of full QCD at nonzero chemical potential have been presented [4–6]. While these initially are carried out in specific parameter domains, the method holds the possibility to provide first principles simulations for any value of the chemical potential, even with low temperature and light quark masses.

The introduction of chiral random matrix theory [7–9] at nonzero chemical potential [10,11] has led to a number of analytic insights into the nonperturbative dynamics of dense strongly interacting matter and the effect of the sign problem [10–14]. In [15], chiral random matrix theory was used to emphasize the potential problem which the complex Langevin faces in simulations of QCD at low temperature and light quark masses.

In this paper we demonstrate that the complex Langevin approach can solve the sign problem in chiral random matrix theory. This is relevant for QCD at low temperature and light quark masses since chiral random matrix theory [7–11] and full QCD share a number of properties: The integral formulation of the partition function in both cases includes the determinant of a Dirac operator, and the flavor symmetries and explicit breaking thereof are identical. QCD and chiral random matrix theory, therefore, have the same low-energy theory in the microscopic limit, namely chiral perturbation theory at leading order in the ϵ domain [7,16–18]. Moreover, the anti-Hermiticity of the Dirac operators is in both cases broken by the chemical potential. This is particularly relevant for the present study, since it implies that the average of the phase factor of the fermion determinant in QCD and chiral random matrix theory have the same analytic form of the exponential suppression in the limit of large volume/size of the matrix [13]. In other words, the sign problem in QCD for light quarks at low temperature and in chiral random matrix theory is equally severe.

In the physical domain where chiral random matrix theory and QCD share the same low-energy limit, both partition functions are independent of the chemical potential μ. This is natural as the partition function is dominated by pions which have zero quark charge. The measures in the partition functions are, however, strongly μ dependent. The numerical problem of realizing the μ independence in both cases becomes particularly challenging once the chemical potential exceeds half of the pion mass ($\mu > m_\pi/2$); see e.g. [13].

In this paper we show that the complex Langevin provides a method to numerically simulate chiral random matrix theory, even in the domain of $\mu > m_\pi/2$. The success compared to the first study [15] is established through a shift of the matrix variables in the integrant as well as by using a polar representation for the new matrix elements.

The advantage of simulating chiral random matrix theory compared to full QCD is that we have exact analytical solutions against which to test the numerics. Tests of this kind are imperative since the complex Langevin is not guaranteed to provide the correct solutions; see for example [19,20]. One potential problem particularly relevant for QCD is that the fermion determinant renders the action nonholomorphic [15]; existing proofs of correct convergence [21–23], therefore, do not apply directly.

As demonstrated in [15,24], the complex Langevin may lead to the wrong results if the argument of the logarithm

(the fermion determinant in QCD and in chiral random matrix theory) frequently circles the origin. In [25] a practical proposal was given in order to circumvent this problem: By initially decreasing the quark mass with the Langevin time, it was suggested that it might be possible to reach the desired value of the quark mass without frequent circulations of the origin by the fermion determinant. Here we test this proposal and show that it is indeed the case within chiral random matrix theory.

The results are presented as follows: In the next section the chiral random matrix theory is defined and the relevant analytic results are stated. Then in Sec. II A the parametrization of the matrix elements is chosen and we explicitly compute the Langevin drift. Section II A presents the numerical results obtained and the proposal to work with an initially Langevin-time-dependent quark mass is tested. We draw conclusions and provide an outlook in Sec. IV.

II. CHIRAL RANDOM MATRIX THEORY

The chiral random matrix theory we will simulate with the complex Langevin has the partition function [11,26]

$$Z_N^{N_f}(m) = \int d\Phi_1 d\Phi_2 \det{}^{N_f}(D_\mu + m) e^{-2N\mathrm{Tr}[\Phi_1^\dagger\Phi_1 + \Phi_2^\dagger\Phi_2]}, \tag{1}$$

where the random matrix analogue of the Dirac operator is

$$D_\mu + m = \begin{pmatrix} m & e^\mu\Phi_1 - e^{-\mu}\Phi_2^\dagger \\ -e^{-\mu}\Phi_1^\dagger + e^\mu\Phi_2 & m \end{pmatrix}. \tag{2}$$

The integration variables Φ_1 and $\Phi_2^\dagger$ are complex $N \times (N+\nu)$ matrices, m and μ are the quark mass and chemical potential parameters and N_f is the number of quark fields which have been integrated out. The integer ν is the topological index, i.e. the number of exact zero eigenvalues of D_μ. In the microscopic limit where mN and $\mu^2 N$ are fixed as $N \to \infty$, this random matrix partition function is equivalent to that of chiral perturbation theory in the ϵ domain [11,17,18]. This limit also allow us to identify the relation between the random matrix parameters N, m and μ and the physical four volume, quark mass and chemical potential, [11,27,28],

$$2mN \leftrightarrow m\Sigma V \quad \text{and} \quad 2\mu^2 N \leftrightarrow \mu^2 F_\pi^2 V, \tag{3}$$

where Σ is the chiral condensate and F_π is the pion decay constant. In the quenched and the phase-quenched theories, a phase transition takes place at $\mu = m_\pi/2$. Using the Gell-Mann-Oakes-Renner relation, we can rewrite this as $\mu^2 F_\pi^2 V = m\Sigma V/2$, which in the chiral random matrix variables translates to $2\mu^2 = m$.

For the numerical test of the complex Langevin below, we will naturally work with finite N. It is, therefore, of great practical value that the partition function (1) can be computed analytically for all values of N_f and N [11,26],

$$Z_N^{N_f}(m) = \frac{1}{(2m)^{1/2N_f(N_f-1)}} \det\left[\left(\frac{d}{dm}\right)^a L_{N+b}^{(\nu)}(-nm^2)\right]_{a=0,\ldots,N_f-1;b=0,\ldots,N_f-1}, \tag{4}$$

where $L_k^{(\nu)}(x)$ is the generalized Laguerre polynomial. From this compact expression for the partition function, we obtain the mass-dependent chiral condensate

$$\Sigma_N^{N_f}(m) = \frac{1}{N_f}\frac{1}{N}\frac{1}{Z_N^{N_f}(m)}\frac{d}{dm} Z_N^{N_f}(m). \tag{5}$$

Note that, as discussed in the Introduction, the partition function is independent of the chemical potential even though the weight in the integral representation (1) is heavily μ dependent.

A. Complex Langevin dynamics

When the action is complex it is natural to generalize real Langevin dynamics [29] by complexifying the fields and define a complexified Langevin dynamics [30,31] through the gradient of the action.

In order to set up the complex Langevin dynamics for the chiral random matrix theory, we first express the partition function (1)

$$Z_N^{N_f}(m) = \int d\Phi_1 d\Phi_2 \exp(-S), \tag{6}$$

in terms of the action

$$S = 2N\mathrm{Tr}[\Phi_1^\dagger\Phi_1 + \Phi_2^\dagger\Phi_2] - N_f\mathrm{Tr}[\log(m^2 - XY)], \tag{7}$$

where

$$X \equiv e^\mu\Phi_1 - e^{-\mu}\Phi_2^\dagger$$
$$Y \equiv -e^{-\mu}\Phi_1^\dagger + e^\mu\Phi_2. \tag{8}$$

Note the appearance of the logarithm of the fermion determinant in the action.

Next we choose to parametrize the elements of the complex $N \times (N+\nu)$ matrices Φ_1 and Φ_2 as

$$(\Phi_1)_{ij} = r_{1,ij}e^{i\theta_{1,ij}} \qquad (\Phi_2)_{ji} = r_{2,ji}e^{i\theta_{2,ji}}, \tag{9}$$

where $i = 1,\ldots,N$ and $j = 1,\ldots,N+\nu$. In the complex Langevin dynamics the $4N(N+\nu)$ real variables $r_{1,ij}$, $\theta_{1,ij}$,

$r_{2,ij}$, $\theta_{2,ij}$ will be complexified. The motivation for the choice of parametrization (9) is that the μ independence of the partition function can be achieved if the Langevin process, in effect, shifts the integration contour of the $\theta_{1,ij}$ and $\theta_{2,ij}$ variables by $i\mu$ into the complex plane while the radial variables $r_{1,ij}$ and $r_{2,ij}$ are attracted to the real axis.

In the parametrization (9), the Gaussian term is simply

$$\mathrm{Tr}[\Phi_1^\dagger\Phi_1+\Phi_2^\dagger\Phi_2]=\sum_{ij} r_{1,ij}^2+r_{2,ji}^2, \tag{10}$$

and the action is, thus,

$$S=-\sum_{ij}\log(r_{1,ij})+\log(r_{2,ji})-\log\det(m^2-XY) + 2N\sum_{ij} r_{1,ij}^2+r_{2,ji}^2, \tag{11}$$

with

$$\begin{aligned} X_{ij} &= e^{\mu+i\theta_{1,ij}}r_{1,ij}-e^{-\mu-i\theta_{2,ji}}r_{2,ji}Y_{ij}\\ &= -e^{-\mu-i\theta_{1,ji}}r_{1,ji}+e^{\mu+i\theta_{2,ij}}r_{2,ij}. \end{aligned} \tag{12}$$

The $\log(r_{1,ij})$ and $\log(r_{2,ji})$ terms are from the Jacobian for the change to polar variables.

The Langevin dynamics is given by the equations

$$\begin{aligned} r_{1,mn}^{(t+1)} &= r_{1,mn}^{(t)}-\frac{\partial S}{\partial r_{1,mn}}dt+\sqrt{dt}\eta(t)r_{2,mn}^{(t+1)}\\ &= r_{2,mn}^{(t)}-\frac{\partial S}{\partial r_{2,mn}}dt+\sqrt{dt}\eta(t)\theta_{1,mn}^{(t+1)}\\ &= \theta_{1,mn}^{(t)}-\frac{\partial S}{\partial \theta_{1,mn}}dt+\sqrt{dt}\eta(t)\theta_{2,mn}^{(t+1)}\\ &= \theta_{2,mn}^{(t)}-\frac{\partial S}{\partial \theta_{2,mn}}dt+\sqrt{dt}\eta(t), \end{aligned} \tag{13}$$

where the derivatives are to be evaluated at Langevin time t, and η is a real Gaussian white noise,

$$\langle\eta(t)\eta(t')\rangle=2\delta(t-t'). \tag{14}$$

The next step is to compute the detailed form of the drift terms which enters the Langevin equations. With the notation

$$P^{-1}\equiv(m^2-XY)^{-1}, \tag{15}$$

we obtain

$$\begin{aligned} -\frac{\partial S}{\partial\theta_{1,mn}} &= -N_f[(P^{-1})_{ki}\partial_{\theta_{1,mn}}(X_{ij}Y_{jk})]\\ &= -N_f[P_{ki}^{-1}(ie^{\mu+i\theta_{1,mn}}r_{1,mn}\delta_{mi}\delta_{nj}Y_{jk}+iX_{ij}\delta_{nj}\delta_{mk}e^{-\mu-i\theta_{1,mn}}r_{1,mn})]\\ &= -iN_f(e^{\mu+i\theta_{1,mn}}r_{1,mn}P_{km}^{-1}Y_{nk}+e^{-\mu-i\theta_{1,mn}}r_{1,mn}P_{mi}^{-1}X_{in})\\ &= -iN_f[e^{\mu+i\theta_{1,mn}}r_{1,mn}((YP^{-1})^{\mathrm{T}})_{mn}+e^{-\mu-i\theta_{1,mn}}r_{1,mn}(P^{-1}X)_{mn}], \end{aligned} \tag{16}$$

while for the radial variable we have

$$\begin{aligned} -\frac{\partial S}{\partial r_{1,mn}} &= -4Nr_{1,mn}+1/r_{1,mn}-N_f[(P^{-1})_{ki}\partial_{r_{1,mn}}(X_{ij}Y_{jk})]\\ &= -4Nr_{1,mn}+1/r_{1,mn}-N_f[P_{ki}^{-1}(e^{\mu+i\theta_{1,mn}}\delta_{mi}\delta_{nj}Y_{jk}-X_{ij}\delta_{nj}\delta_{mk}e^{-\mu-i\theta_{1,mn}})]\\ &= -4Nr_{1,mn}+1/r_{1,mn}-N_f(e^{\mu+i\theta_{1,mn}}P_{km}^{-1}Y_{nk}-e^{-\mu-i\theta_{1,mn}}P_{mi}^{-1}X_{in})\\ &= -4Nr_{1,mn}+1/r_{1,mn}-N_f[e^{\mu+i\theta_{1,mn}}((YP^{-1})^{\mathrm{T}})_{mn}-e^{-\mu-i\theta_{1,mn}}(P^{-1}X)_{mn}]. \end{aligned} \tag{17}$$

Similarly, for the angular and radial variables from Φ_2, we have

$$\begin{aligned} -\frac{\partial S}{\partial\theta_{2,mn}} &= -N_f[(P^{-1})_{ki}\partial_{\theta_{2,mn}}(X_{ij}Y_{jk})]\\ &= -N_f[P_{ki}^{-1}(ie^{-\mu-i\theta_{2,mn}}r_{2,mn}\delta_{ni}\delta_{mj}Y_{jk}+iX_{ij}\delta_{mj}\delta_{nk}e^{\mu+i\theta_{2,mn}}r_{2,mn})]\\ &= -iN_f(e^{-\mu-i\theta_{2,mn}}r_{2,mn}P_{kn}^{-1}Y_{mk}+e^{\mu+i\theta_{2,mn}}r_{2,mn}P_{ni}^{-1}X_{im})\\ &= -iN_f[e^{-\mu-i\theta_{2,mn}}r_{2,mn}(YP^{-1})_{mn}+e^{\mu+i\theta_{2,mn}}r_{2,mn}((P^{-1}X)^{\mathrm{T}})_{mn}] \end{aligned} \tag{18}$$

and

$$
\begin{aligned}
-\frac{\partial S}{\partial r_{2,mn}} &= -4Nr_{2,mn} + 1/r_{2,mn} - N_f[(P^{-1})_{ki}\partial_{r_{2,mn}}(X_{ij}Y_{jk})] \\
&= -4Nr_{2,mn} + 1/r_{2,mn} - N_f[P^{-1}_{ki}(-e^{-\mu-i\theta_{2,mn}}\delta_{ni}\delta_{mj}Y_{jk} + X_{ij}\delta_{mj}\delta_{nk}e^{\mu+i\theta_{2,mn}})] \\
&= -4Nr_{2,mn} + 1/r_{2,mn} - N_f(-e^{-\mu-i\theta_{2,mn}}P^{-1}_{kn}Y_{mk} + e^{\mu+i\theta_{2,mn}}P^{-1}_{ni}X_{im}) \\
&= -4Nr_{2,mn} + 1/r_{2,mn} - N_f[-e^{-\mu-i\theta_{2,mn}}(YP^{-1})_{mn} + e^{\mu+i\theta_{2,mn}}((P^{-1}X)^{\mathrm{T}})_{mn}]. \qquad (19)
\end{aligned}
$$

Note that we have ignored the cut of the logarithm and simply used the standard form for the derivative of the log when the argument is real and positive. This has potential consequences for the Langevin process [15] in particular if the argument of the log frequently circles the origin of the complex plane. We will return to this point in Sec. III A below.

The Langevin dynamics presented above differs in two ways from that used in [15]. First, the realization (1) of the chiral random matrix theory partition function is related to the partition function used in [15] (see Eq. (4.1) therein) by a change of the matrices which enter as integration variables (see also the Appendix of [26]). Second, the parametrization of the matrix elements (9) used here is different from that used in [15]. Both changes are necessary for the success of the simulations presented below.

III. SIMULATIONS

In order to test the complex Langevin algorithm presented above, we have run a series of numerical simulations. The central observable of interest is the chiral condensate for which the analytic prediction is given in Eq. (5). This observable is not only relevant for the nonperturbative physics but also highly sensitive to the sign problem, since the phase-quenched chiral condensate takes a drastically different form in the region of $m < 2\mu^2$; see e.g. [15] for plots thereof.

To compute the chiral condensate, we start the Langevin process in a random configuration from the original (not complexified) quenched ensemble. The Langevin process is then run for a period, $2T$, in time steps of dt, and on the latter half of the trajectory we compute

$$
\Sigma(m) = \frac{1}{N_f}\frac{1}{N}\frac{1}{T}\sum_{t=T+dt}^{2T}\mathrm{ReTr}\,\frac{1}{D_\mu^{(t)}+m}\,dt, \qquad (20)
$$

where $D_\mu^{(t)} + m$ is the Dirac operator (2) evaluated for the complexified fields generated in (16)–(19) at Langevin time t. The first half, T, of the period allows the Langevin process to react to the initial condition and cool towards equilibrium.

With increasing size of the matrices, we have found it convenient to implement adaptive step-size [19,32], since the $1/r$ terms in the drift can lead to large excursions unless dt is sufficiently small. Results for the chiral condensate for $N = 20$, $\mu = 1$, $2T = 2000$, $\nu = 0$ and adaptive step-size are shown in Fig. 1. Displayed are the numerical results for $N_f = 1$, 2 and 3 as well as the analytic predictions. The numerical code used is implemented within the PYTHON framework where the NUMPY packages allow for fast exact matrix inversion. We observe that the Langevin process is able to reproduce the expected mass dependence throughout the range of values for m with all three values of N_f. Note that $m < 2\mu^2$ throughout the range displayed. The convergence is equally good for larger values of m.

Next we have tested the Langevin dynamics for nonzero topological index ν. In Fig. 2 the numerical results for $\nu = 0$, 1 and 2 with adaptive step-size, $N_f = 2$, $N = 20$, $2T = 2000$, are plotted against the analytic curves. The numerical data again follow the expected curves and demonstrate that the topological zero modes create no obstacles for the complex Langevin algorithm in chiral random matrix theory.

In order to gain insights in the dynamics of these successful simulations, we have monitored the values of the variables throughout the Langevin process: The angular variables $\theta_{1,ij}$ and $\theta_{2,ij}$ are effectively shifted by $i\mu$ into the complex plane while the $r_{1,ij}$ and $r_{2,ij}$ are attracted toward the real axis. This cancels the μ dependence of the chiral condensate, as was indeed the motivation for the choice of

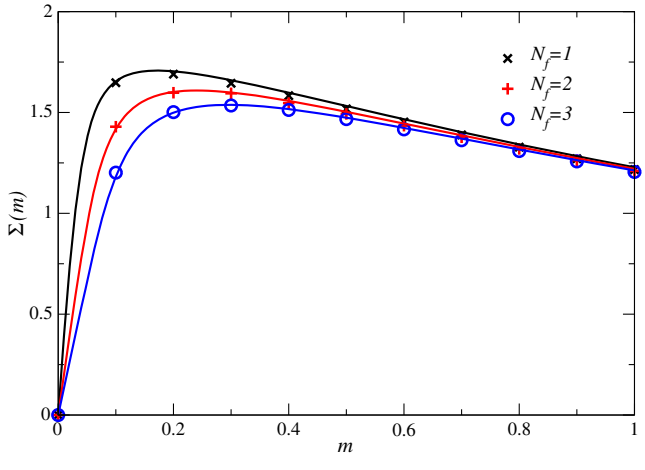

FIG. 1 (color online). The chiral condensate as a function of the quark mass for one, two and three dynamical flavors. The full lines are the exact analytic predictions, and the points are the results of the complex Langevin dynamics with adaptive step-size. The parameters chosen for the plot are $N = 20, \mu = 1, \nu = 0$ and $2T = 2000$.

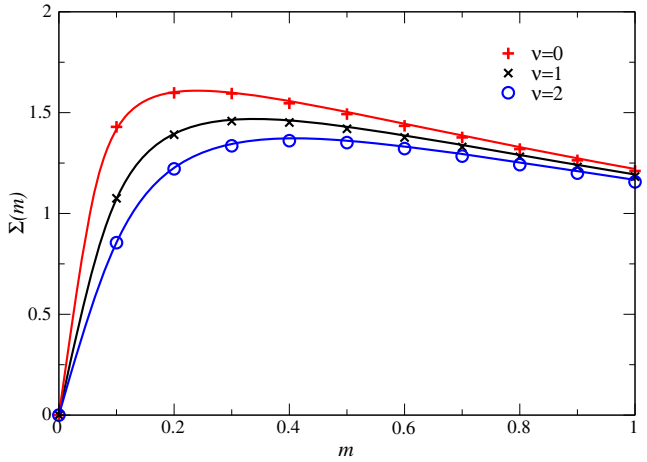

FIG. 2 (color online). The chiral condensate as a function of the quark mass for $\nu = 0, 1, 2$ with $N_f = 2$, $N = 20$, $\mu = 1$ and $\nu = 0$. The data points are obtained with the complex Langevin using an adaptive step-size and the full lines are the predictions (5).

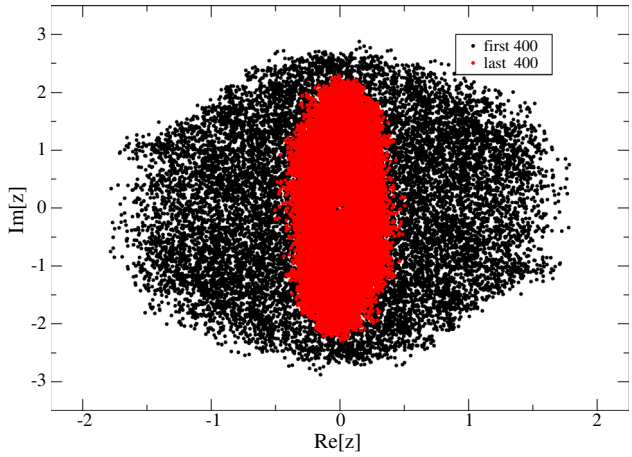

FIG. 4 (color online). The eigenvalues of the Dirac operator in the complex plane: *black* for the first 400 time steps and *red* for the final 400 time steps. Parameters used are $N = 20$, $N_f = 2$, $\mu = 1$, $m = 1$, $\nu = 0$ and 60000 adaptive steps. Note that the quark mass is initially well inside the eigenvalue distribution.

parametrization (9). An example of the flow of the variable is shown in Fig. 3. The band is the average of the imaginary part of the elements in θ_1 with the errors given by the square root of the variance.

The flows of the variables manifest themselves also in the distribution of the Dirac eigenvalues. In Fig. 4 the eigenvalues of the Dirac operator on the initial 400 configurations are plotted in black along with the eigenvalues of the final 400 configurations out of 60000 adaptive steps. The value of the quark mass, $m = 1$, is well within the initial eigevalue distribution; however, with Langevin time the Dirac eigenvalues move inside the quark mass. As this happens, the fluctuations of the phase of the fermion determinant are damped; see Fig. 5.

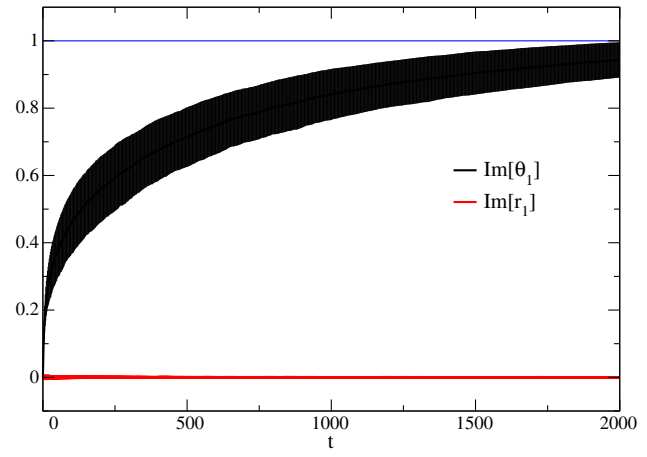

FIG. 3 (color online). The average of the imaginary part of the angular variable θ_1 and the average of the imaginary part of the radial variable r_1. As a function of the Langevin time t, the angular variable flows towards $\mu = 1$, marked by the thin vertical line, while the radial variable remains on the real axis within the errors. The error bars are given by the square root of the variance. The parameters in the simulation are $\nu = 0$, $N_f = 2$, $N = 20$, $\mu = 1$, $m = 1$ and $\nu = 0$.

A. Decreasing the quark mass with Langevin time

In large scale simulations it becomes exceedingly hard to invert the Dirac operator if the quark mass is inside the eigenvalue distribution. Moreover, in this case the fermion determinant is likely to circulate the origin frequently

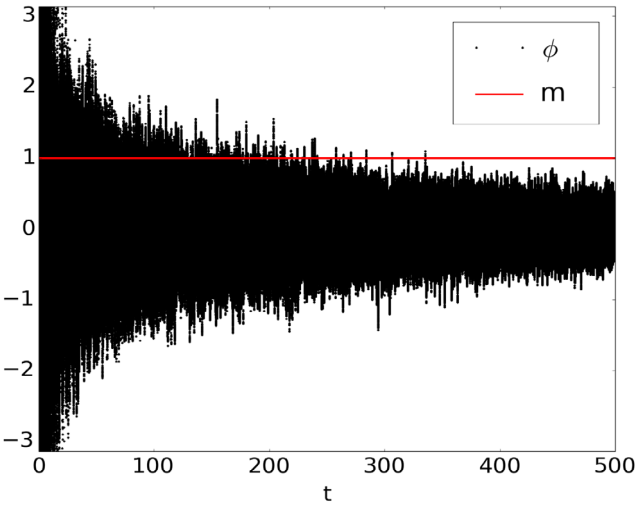

FIG. 5 (color online). The argument, ϕ, of the phase of the fermion determinant as a function of Langevin time, for $m = 1$, $\mu = 1$, $N = 20$, $N_f = 2$ and $\nu = 0$. Initially the fermion determinant frequently circles the origin but with the Langevin time the Dirac eigenvalues flow inside the quark mass and the fluctuations of the fermion determinant are damped. The fixed value of the quark mass throughout the run is indicated bu the horizontal red line.

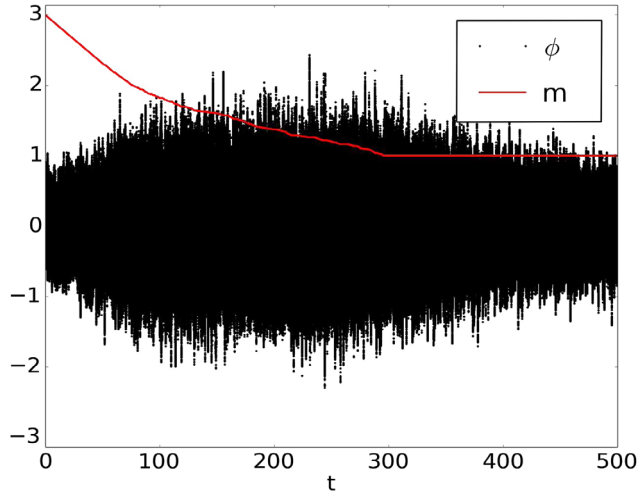

FIG. 6 (color online). The argument of the phase of the fermion determinant along the Langevin trajectory. With the Langevin-time-dependent quark mass (thin red curve), the fermion determinant does not circle the origin during the Langvin process. Here $\mu = 1$, $N = 20$, $N_f = 2$, $\nu = 0$ and the initial value of the quark mass, 3, is outside the cloud of Dirac eigenvalues. As the quark mass reaches the desired value $m = 1$, it is kept fixed and the measurement of the chiral condensate can be performed.

(when the quark mass is inside the Dirac eigenvalues the phase of the fermion determinant is distributed according to a Lorentzian distribution [33]) and, hence, ignoring the cut of the logarithm is not necessarily justified [15]. In order to circumvent these issues, it was proposed in [25] to allow the quark mass to decrease with the Langevin time t. The proposal is to start from an initial value of the quark mass which is outside the Dirac eigenvalue distribution. With Langevin time the quark mass is then slowly decreased towards the desired value. In this way it is possible that the quark mass remains outside the distribution of the eigenvalues of the Dirac operator and that the fermion determinant does not circulate the origin at any given time throughout the Langevin process. Once the desired quark mass is reached, all previous configurations are discarded from the measurement of the given observable.

Here we test this proposal within the Langevin process for chiral random matrix theory. What we will show is that with a Langevin-time-dependent quark mass, the fluctuations of the phase of the random matrix fermion determinant can be constrained for the entire Langevin trajectory. We start the Langevin process on a random configuration from the original quenched ensemble (not complexified) and pick a value of the quark mass parameter which is safely outside the Dirac eigenvalues, i.e. $m > 2\mu^2$. The quark mass is reduced in steps proportional to the time step, unless the angle of the determinant has been above 1.5 within the last 1000 time steps. In that case we keep the quark mass constant to allow the Langevin dynamics to dampen the fluctuations of the phase of the determinant. This procedure is repeated until m reaches the desired value, here 1; see Fig. 6. We observe that with Langevin time it is possible to decrease the quark mass such that the fermion determinant at no point during the Langevin trajectory circulates the origin. The potential problems with the log of the fermion determinant can therefore safely be ignored.

IV. CONCLUSIONS

We have demonstrated that the complex Langevin can simulate chiral random matrix theory at nonzero chemical potential even in the range corresponding to $\mu > m_\pi/2$. The success of the complex Langevin method in chiral random matrix theory was established by (1) a change of integration matrices and (2) a polar parametrization of these variables before complexification. This choice of variables was inspired by taking the perspective of the eigenvalues of the Dirac operator evaluated on the complexified configurations. As shown in [25], the Dirac spectrum of complex Langevin simulations must be vastly different from that with real configurations. In the application of the complex Langevin to chiral random matrix theory, the natural solution is to realize an effective anti-Hermitization of the Dirac operator through the complexification of the matrix elements. The choice of matrix integration variables and the polar parametrization of the elements herein were handpicked to optimize the chance for the complex Langevin to realize this effective anti-Hermitization. Indeed, we have checked that the success of the complex Langevin in chiral random matrix theory is established through an effective shift into the complex plane of the angular part of the matrix elements. This smoothly connects the initial non-Hermitian random matrix Dirac operator to an anti-Hermitian counterpart at large Langevin time. For a discussion of the possibility to realize a similar scenario in the context of full QCD, see [25].

As the chiral random matrix Dirac operator shares the chiral symmetries of the QCD Dirac operator, it allows us to address several properties directly relevant for QCD. In particular, we have tested the proposal of [25] in which the quark mass is initially Langevin time dependent: With an adaptive step-size and a Langevin-time-dependent quark mass, we have demonstrated that it is possible to simulate the chiral random matrix theory at small mass (such that $m_\pi < 2\mu$) without the determinant frequently circulating the origin. This minimizes the potential problems due to the nonholomorphic nature of the action in the presence of a fermion determinant. Furthermore, it ensures that inversions of the Dirac operator only appear with the quark mass outside the eigenvalues of the Dirac operator.

It would be most interesting to understand if the effect of a Langevin-time-dependent quark mass in complex Langevin simulations of full QCD is beneficial, in particular at low temperature and light quark mass. As an intermediate step a Langevin-time-dependent quark mass

could also be implemented for the Thirring model [34]. Another possible direction is to use the eigenvalue representation of the chiral random matrix partition function as the basis for the Langevin process. Such an approach has already led to new insights for QCD in one dimension [35].

ACKNOWLEDGMENTS

The work of A. M. is supported by the interdisciplinary UCPH 2016 Grant "Social Fabric," and the work of K. S. is supported by the Sapere Aude program of the Danish Council for Independent Research.

[1] G. Aarts, *Proc. Sci.*, LATTICE2012 (2012) 017.
[2] P. de Forcrand, *Proc. Sci.*, LAT2009 (2009) 010.
[3] K. Splittorff, *Proc. Sci.*, LAT2006 (2006) 023.
[4] D. Sexty, Phys. Lett. B **729**, 108 (2014).
[5] D. Sexty, arXiv:1410.8813.
[6] G. Aarts, E. Seiler, D. Sexty, and I. O. Stamatescu, Phys. Rev. D **90**, 114505 (2014).
[7] E. V. Shuryak and J. J. M. Verbaarschot, Nucl. Phys. **A560**, 306 (1993).
[8] J. J. M. Verbaarschot and I. Zahed, Phys. Rev. Lett. **70**, 3852 (1993).
[9] J. J. M. Verbaarschot, Phys. Rev. Lett. **72**, 2531 (1994).
[10] M. A. Stephanov, Phys. Rev. Lett. **76**, 4472 (1996).
[11] J. C. Osborn, Phys. Rev. Lett. **93**, 222001 (2004).
[12] A. M. Halasz, A. D. Jackson, R. E. Shrock, M. A. Stephanov, and J. J. M. Verbaarschot, Phys. Rev. D **58**, 096007 (1998).
[13] K. Splittorff and J. J. M. Verbaarschot, Phys. Rev. Lett. **98**, 031601 (2007); Phys. Rev. D **75**, 116003 (2007); **77**, 014514 (2008).
[14] J. C. Osborn, K. Splittorff, and J. J. M. Verbaarschot, Phys. Rev. Lett. **94**, 202001 (2005); Phys. Rev. D **78**, 065029 (2008).
[15] A. Mollgaard and K. Splittorff, Phys. Rev. D **88**, 116007 (2013).
[16] J. J. M. Verbaarschot and T. Wettig, Annu. Rev. Nucl. Part. Sci. **50**, 343 (2000).
[17] G. Akemann, Int. J. Mod. Phys. A **22**, 1077 (2007).
[18] F. Basile and G. Akemann, J. High Energy Phys. 12 (2007) 043.
[19] J. Ambjorn, M. Flensburg, and C. Peterson, Nucl. Phys. **B275**, 375 (1986).
[20] G. Aarts and F. A. James, J. High Energy Phys. 08 (2010) 020.
[21] G. Aarts, E. Seiler, and I.-O. Stamatescu, Phys. Rev. D **81**, 054508 (2010).
[22] G. Aarts, F. A. James, E. Seiler, and I.-O. Stamatescu, Eur. Phys. J. C **71**, 1756 (2011).
[23] G. Aarts, F. A. James, E. Seiler, and I.-O. Stamatescu, *Proc. Sci.*, LATTICE2011 (2011) 197.
[24] J. Greensite, Phys. Rev. D **90**, 114507 (2014).
[25] K. Splittorff, arXiv:1412.0502.
[26] J. Bloch, F. Bruckmann, M. Kieburg, K. Splittorf,f, and J. J. M. Verbaarschot, Phys. Rev. D **87**, 034510 (2013).
[27] K. Splittorff and J. J. M. Verbaarschot, Nucl. Phys. **B683**, 467 (2004).
[28] G. Akemann, J. C. Osborn, K. Splittorf,f, and J. J. M. Verbaarschot, Nucl. Phys. **B712**, 287 (2005).
[29] P. H. Damgaard and H. Huffel, Phys. Rep. **152**, 227 (1987).
[30] G. Parisi, Phys. Lett. B **131**, 393 (1983).
[31] J. R. Klauder, Acta Phys. Austriaca **25**, 251 (1983).
[32] G. Aarts, F. A. James, E. Seiler, and I. O. Stamatescu, Phys. Lett. B **687**, 154 (2010).
[33] M. P. Lombardo, K. Splittorff, and J. J. M. Verbaarschot, Phys. Rev. D **80**, 054509 (2009).
[34] J. M. Pawlowski and C. Zielinski, Phys. Rev. D **87**, 094509 (2013); **87**, 094503 (2013).
[35] G. Aarts and K. Splittorff, J. High Energy Phys. 08 (2010) 017.